Cancer Research

β-Lapachone Micellar Nanotherapeutics for Non–Small Cell Lung Cancer Therapy

Elvin Blanco[1], Erik A. Bey[1,2], Chalermchai Khemtong[1], Su-Geun Yang[1], Jagadeesh Setti-Guthi[1], Huabing Chen[1], Chase W. Kessinger[1], Kevin A. Carnevale[3], William G. Bornmann[4], David A. Boothman[1,2], and Jinming Gao[1]

Abstract

Lung cancer is the leading cause of cancer-related deaths with current chemotherapies lacking adequate specificity and efficacy. β-Lapachone (β-lap) is a novel anticancer drug that is bioactivated by NAD(P)H:quinone oxidoreductase 1, an enzyme found specifically overexpressed in non–small cell lung cancer (NSCLC). Herein, we report a nanotherapeutic strategy that targets NSCLC tumors in two ways: (*a*) pharmacodynamically through the use of a bioactivatable agent, β-lap, and (*b*) pharmacokinetically by using a biocompatible nanocarrier, polymeric micelles, to achieve drug stability, bioavailability, and targeted delivery. β-Lap micelles produced by a film sonication technique were small (~30 nm), displayed core-shell architecture, and possessed favorable release kinetics. Pharmacokinetic analyses in mice bearing subcutaneous A549 lung tumors showed prolonged blood circulation ($t_{1/2}$, ~28 h) and increased accumulation in tumors. Antitumor efficacy analyses in mice bearing subcutaneous A549 lung tumors and orthotopic Lewis lung carcinoma models showed significant tumor growth delay and increased survival. In summary, we have established a clinically viable β-lap nanomedicine platform with enhanced safety, pharmacokinetics, and antitumor efficacy for the specific treatment of NSCLC tumors. *Cancer Res; 70(10); 3896–904. ©2010 AACR.*

Introduction

Lung cancer currently accounts for ~30% of cancer-related deaths in both males and females in the United States (1). A current trend in cancer chemotherapy involves the identification of exploitable molecular targets unique to cancer cells for tumor-specific drug therapy. β-Lapachone (β-lap) is a novel anticancer agent whose mechanism of action is highly dependent on the enzyme NAD(P)H:quinone oxidoreductase 1 (NQO1), a flavoprotein found overexpressed in non–small cell lung cancer (NSCLC; ref. 2). In cells overexpressing NQO1, β-lap undergoes a futile cycle resulting in reactive oxygen species (ROS) generation (3). These ROS cause DNA single-strand breaks, hyperactivation of poly(ADP-ribose) polymerase-1 (PARP-1; ref. 4), loss of NAD^+ and ATP pools, and a unique pattern of cell death referred to as "programmed necrosis" or "necroptosis" (Fig. 1; ref. 5). Necroptosis is a unique form of cell death that has attributes from both apoptosis (e.g., terminal deoxynucleotidyl transferase–mediated dUTP nick end labeling positive and chromatin and nuclear condensation) and necrosis (e.g., caspase and energy independent). Cell death occurs specifically in tumor tissues overexpressing NQO1, whereas normal tissues and organs with endogenous low levels of the enzyme are spared. This antitumor mechanism was shown to be effective in breast (6), prostate (7), and NSCLC cells (4). Although promising, the poor water solubility (0.038 mg/mL) and nonspecific drug distribution of β-lap limit its clinical potential. Early attempts at formulating β-lap for the clinics focused on complexation with cyclodextrins such as hydroxypropyl-β-cyclodextrin (HPβ-CD). The resulting formulation, β-lap·HPβ-CD (i.e., ARQ501), showed a 400-fold increase in solubility (8) but underwent unsuccessful clinical trials in a variety of cancers (9–12). The reason for failure includes dose-limiting toxicity in the form of hemolytic anemia and nonspecific drug distribution, resulting in poor antitumor efficacy.

Currently, nanomedicine, or the use of nanoscale (1–100 nm) constructs for diagnostic and therapeutic applications, represents an innovative trend in cancer care (13, 14). Advancements in nanomaterials and nanotechnology have paved the way for several carriers such as liposomes (15), dendrimers (16), and micelles (17, 18). Polymeric micelles, or nanosized (~10–100 nm) supramolecular constructs composed of amphiphilic block copolymers, are emerging as powerful drug delivery vehicles for hydrophobic drugs.

Authors' Affiliations: [1]Departments of Pharmacology and [2]Radiation Oncology, Simmons Comprehensive Cancer Center, University of Texas Southwestern Medical Center at Dallas, Dallas, Texas; [3]Departments of Pathology, Microbiology, and Immunology, University of South Carolina, Columbia, South Carolina; and [4]Department of Experimental Therapeutics, University of Texas M.D. Anderson Cancer Center, Houston, Texas

Note: Supplementary data for this article are available at Cancer Research Online (http://cancerres.aacrjournals.org/).

E. Blanco and E.A. Bey contributed equally to this work.

Corresponding Authors: Jinming Gao or David A. Boothman, University of Texas Southwestern Medical Center at Dallas, 5323 Harry Hines Boulevard, Dallas, TX 75390-8807. Phone: 214-645-6370; Fax: 214-645-6347; E-mail: jinming.gao@utsouthwestern.edu or david.boothman@utsouthwestern.edu.

doi: 10.1158/0008-5472.CAN-09-3995

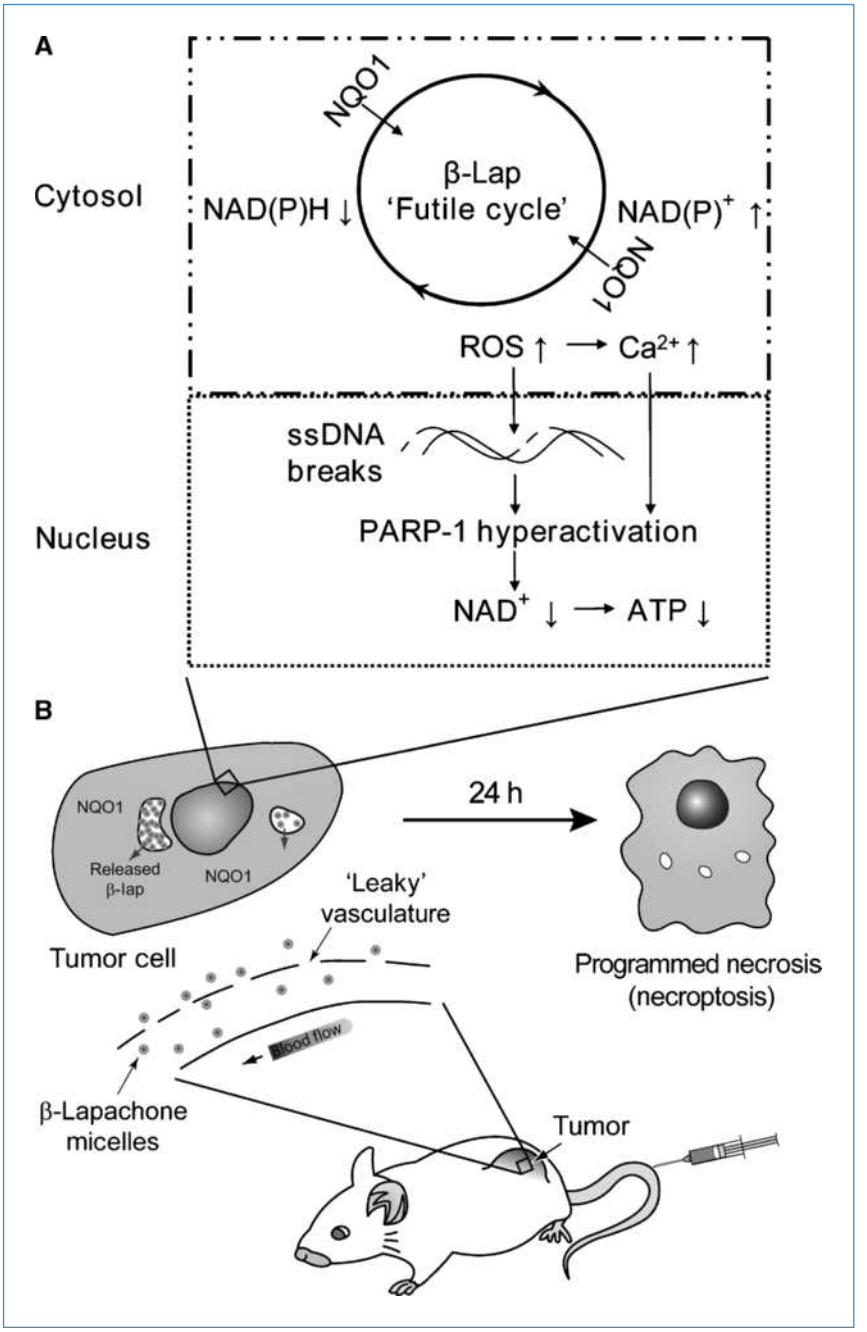

Figure 1. Proposed dual targeting mechanism by β-lap nanotherapeutics. Depicted is a simplified model that summarizes the pharmacokinetic and pharmacodynamic targeting strategy provided by β-lap micelles. A, polymer micelles provide long circulation and reduced drug clearance that enhances accumulation in tumor tissue, wherein micelles are internalized into cells and drug is released. B, tumor cell killing is accomplished through the NQO1-dependent mechanism of action of β-lap, a unique pattern of cell death referred to as programmed necrosis or necroptosis.

Advantages afforded for drug delivery include the presence of an inner core for lipophilic drug entrapment, as well as a hydrophilic outer shell that prevents particle aggregation and opsonization (19). This hinders uptake by the reticuloendothelial system (RES; ref. 20), bestowing them with long circulation times that, combined with their small size, aid in preferential accumulation in tumor tissue through the enhanced permeability and retention (EPR) effect (Fig. 1; refs. 21, 22). These benefits for site-specific drug delivery will facilitate clinical translation of traditional and emerging chemotherapeutic agents with immense cell killing potential but that are otherwise abandoned due to insolubility and toxicity.

In this report, we describe the implementation of polymeric micelles to generate a clinically viable formulation of β-lap as a safe and efficacious nanotherapeutic platform for the treatment of NSCLCs. We hypothesized that β-lap micelles would provide a synergistic pharmacokinetic and pharmacodynamic targeting of NQO1-overexpressing lung tumors (Fig. 1). By using a highly efficient vehicle that ensures tumor accumulation, as well as a cancer-specific agent for NSCLC, a novel treatment strategy may arise that can help combat the disease.

Materials and Methods

Materials. HPβ-CD was obtained from Cyclodextrin Technologies Development, Inc. with >98% purity. β-Lap was synthesized as described (23). PEG5k-PLA5k block copolymer (molecular weight = 10,000 Da) was synthesized by a ring-opening polymerization procedure (24). All organic solvents were analytical grade. β-Lap·HPβ-CD was formulated using a previously published procedure (8). β-Lap micelles were fabricated as described (25). PBS (pH 7.4) was purchased from Fisher Scientific. Mouse LLC lung cancer cells were grown in DMEM with 10% fetal bovine serum, 2 mmol/L L-glutamine, 100 units/mL penicillin, and 100 mg/mL streptomycin at 37°C in a humidified incubator in a 5% CO_2–95% air atmosphere. The A549 and LLC cells were infected with a lentivirus construct that contained the luciferase gene with a cytomegalovirus promoter. Cells were *Mycoplasma*-free.

Preparation of β-lap·HPβ-CD complex and β-lap micelles. β-Lap·HPβ-CD complexes were prepared as described (8), filtered by 0.2-μm nylon filtration, and the concentration of β-lap was determined using UV-Vis spectroscopy [λ_{max} = 257 nm, ε = 105 mL/(cm·mg β-lap)].

A film sonication method was used to produce β-lap micelles (25). Briefly, β-lap and poly(ethylene glycol)-co-poly (D,L-lactic acid) (PEG-PLA [5%, w/w]) were dissolved in acetone and the organic solvent was allowed to evaporate, yielding a solid film. Water was then added and the solution was sonicated for 5 minutes. Drug-loaded polymer micelles were filtered through 0.45-μm nylon filters to remove nonencapsulated drug aggregates, and the micelle solution was stored immediately at 4°C to prevent premature drug release. The solution of micelles was then concentrated by centrifugation (3,000 rpm, 4°C) using Amicon ultracentrifugal filters (molecular weight cutoff = 100 kDa). β-Lap concentration was then determined by lyophilizing a known volume of solution that was redissolved in chloroform and analyzed by UV-Vis as described above.

For radiolabeled polymers used in pharmacokinetic studies, a small amount of MeO-PEG-PLA-OCOC^3H_3 (1%, w/w) was dissolved with PEG-PLA, and β-lap micelles were prepared in a similar method as described above.

Pharmacokinetic analyses of β-lap micelles. All animal procedures adhered to NIH guidelines, following approved protocols by the Institutional Animal Care and Use Committee at the University of Texas Southwestern Medical Center at Dallas. Experiments involving radioactive materials were approved by the Radiation Safety Committee. Pharmacokinetic studies determining blood concentration over time, as well as tissue of distribution of β-lap micelles, were performed in 6- to 8-week-old randomized tumor-bearing female athymic nude mice (~25 g each). Log-phase A549 cells (5×10^6) were injected s.c. into the flanks of mice. Tumor sizes were regularly measured using calipers, and volumes were calculated using the following formula: volume (mm^3) = length × width × width/2. Pharmacokinetic studies were initiated with randomized mice containing average tumor volumes of ~300 mm^3.

β-Lap micelles containing 1% ^{3}H-labeled PEG-PLA were injected into mice via the tail vein. Blood was collected from the ocular vein at various times (1 min to 24 h) after injection. Plasma was isolated and mixed with a tissue solubilizer (1 mL, BTS-450; Beckman) at room temperature for 5 hours followed by addition of liquid scintillation mixture (10 mL), and the mixture was incubated for 12 hours. Biodistribution studies of β-lap micelles in tissues and organs were conducted at various times from 0 to 24 hours. Animals were sacrificed, and organs were harvested, weighed, and resuspended in deionized water. Tissues were subsequently homogenized by adding tissue solubilizer (1 mL), 30% H_2O_2, liquid scintillation mixture, and acetic acid. Radioactive isotope quantities in samples were monitored using a predetermined calibration curve on a Beckman LS 6000 IC liquid scintillation counter. Results were presented as percentage (%) initial dose per gram tissue. All experiments were performed in triplicate, and data were analyzed using a two-compartment pharmacokinetic model (26).

Treatment of subcutaneous A549 lung tumors in mice. A549 xenografts in 6- to 8-week-old female athymic nude mice were prepared as described above. Animals bearing ~200 mm^3 tumors were randomized and used to examine the antitumor efficacy of β-lap·HPβ-CD complexes versus β-lap micelles. Both formulations were i.v. administered to mice (n = 5) every other day for 9 days at doses ranging from 30 to 50 mg/kg. Tumor sizes were measured as described above. At day 30, tumor-bearing mice were imaged using bioluminescence imaging (BLI) for purposes of tumor size comparison. For BLI, animals were placed under anesthesia using isoflurane, and 2.5 mg D-luciferin was s.c. administered. BLI images of mice were captured using a Xenogen Vivovision IVIS Lumina Imager for 30 seconds. For long-term survival studies, animals were sacrificed when tumor volumes reached 1,500 mm^3.

β-Lap efficacy studies using tail vein–induced orthotopic LLC tumors in athymic nude mice. Female athymic mice (~25 g) were injected i.v. with 0.5×10^6 LLC cells via tail vein. It was found by BLI that the injected cells transplanted to the intended site of the lungs to establish the orthotopic lung tumor model. Mice were randomized into two groups (n = 8) for β-lap micelle or control (blank) micelle treatments. Mice were monitored every other day using BLI for tumor growth. Relative light intensity units (from 7.5×10^4 to 3.0×10^5) were used as a marker for tumor initiation in the lungs. Day 0 was designated as initial detection of disease and the day before start of treatment. Animals were treated with 40 mg/kg β-lap micelles administered i.v. via tail vein and repeated five times every other day over 9 days. Animals were monitored daily for survival. In a separate study, mice (n = 3) were administered β-lap micelles or control micelles, and animals were sacrificed at day 9 to examine disease progression via gross inspection and detailed histologic evaluation. Lungs were fixed in 10% formalin overnight and embedded by the Histology Core (Departments of Pathology and Molecular Pathology, University of Texas Southwestern Medical Center). H&E staining was performed on paraffin-embedded 5-μm tissue sections. Whole-mount images of sections were imaged using a Leica DMI6000 inverted microscope. Single images at ×50 (total magnification) were compiled using the Leica Application

Suite computer program to create the final whole-mount image. Total lung area and tumor area were calculated using ImageJ software (NIH).

Statistical analyses. Statistical analyses of survival data and lung tumor areas were performed using GraphPad Prism software. All statistical analyses were two-sided. In the subcutaneous lung tumor model, the effects of each treatment on long-term survival (Kaplan-Meier curves) were analyzed using log-rank (Mantel-Cox) tests, with significance levels of 0.05. Significant differences between orthotopic LLC tumor volumes following micelle or β-lap micelle treatments were estimated using two-tailed *t* tests of unequal variance, where *P* values of ≤0.05 were considered significant. All statistical analyses were performed with assistance and final verification from the Biostatistics Core (Simmons Comprehensive Cancer Center, University of Texas Southwestern Medical Center).

Results

β-Lap was incorporated into PEg-PLA (molecular weight, 10,000 Da) polymer micelles using a film sonication procedure (Fig. 2A; ref. 25). The resulting nanoparticles possessed core-shell morphology and were spherical and highly monodisperse, as verified by transmission electron microscopy (TEM; Fig. 2B). Micellar diameters averaged 26.8 ± 3.2 nm, as measured by dynamic light scattering (Fig. 2C). β-Lap micelles had loading efficiency and density values of 39.8 ± 1.0% and 2.2 ± 0.1%, respectively (25). As reported previously, the release kinetics of β-lap from polymer micelles exhibited diffusion-based release behavior, with 50% drug release within 18 hours, and the majority of drug (>75%) was released over the course of 4 days.

To investigate the safety of β-lap micelles, morbidity and mortality responses were recorded in healthy mice at different doses of β-lap·HPβ-CD complexes or β-lap micelles (Supplementary Table S1). Five i.v. injections every other day of 30 mg/kg β-lap·HPβ-CD resulted in no deaths. However, moderate side effects were observed, with mice experiencing labored breathing and an irregular gait. These symptoms were more intense at higher doses of 40 and 50 mg/kg β-lap·HPβ-CD, yielding severe muscle contractions, labored breathing, and lethality in some cases. A dose of 60 mg/kg β-lap·HPβ-CD resulted in severe morbidity and eventually 100% lethality. In contrast, β-lap micelle doses ranging from 30 to 50 mg/kg did not result in any deaths and had significantly less side effects. Mice injected with 40 and 50 mg/kg of β-lap micelles experienced mild and moderate labored breathing and irregular gait. At 60 mg/kg β-lap micelles, animal reactions were severe and animal deaths (~40%) ensued. As a result of these studies, we concluded that optimal doses of β-lap micelles were in the range of 30 to 50 mg/kg, and a clear safety advantage of β-lap micelles over β-lap·HPβ-CD.

Prior clinical trial data suggested that improved β-lap formulations are necessary to reduce dose-limiting toxicity (e.g., hemolytic anemia) of cyclodextrin-complexed β-lap (9). To investigate this, we compared the percentage (%) of hemolysis of different β-lap formulations (Supplementary Fig. S1). Data show that β-lap·HPβ-CD indeed caused hemolysis, with

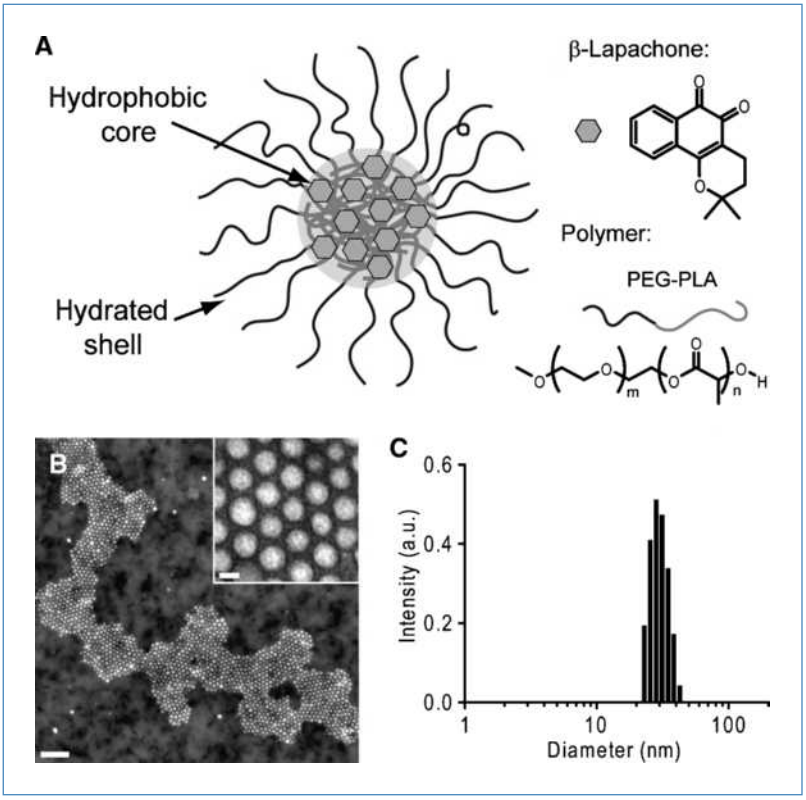

Figure 2. β-Lap micelle characterization. A, schematic of a β-lap polymer micelle with constituent components. B, TEM image of β-lap polymer micelles using 2% phosphotungstic acid as a counterstain. Scale bars, 200 nm (image) and 20 nm (inset). C, histogram of β-lap micelle diameter determined by dynamic light scattering.

concentrations at 1.0 and 1.5 mg/mL β-lap resulting in 47 ± 1% and 52 ± 2% hemolysis, respectively. However, we noted that HPβ-CD alone caused significant hemolysis (94 ± 1%) at HPβ-CD concentrations required to solubilize β-lap at 1.5 mg/mL. Importantly, no measurable hemolysis was observed from β-lap micelles at all concentrations examined.

Exposure of RBCs to β-lap affected hemoglobin (Hb), the major component of RBCs. In samples coincubated with β-lap·HPβ-CD, a blue shift of the Hb λ_{max} was noted from 415 nm to a lower wavelength of 408 nm (Supplementary Fig. S1C), a shift missing in HPβ-CD alone samples. Importantly, this change in λ_{max} of Hb was not apparent in β-lap micelle samples, given their inability to cause cell lysis and release Hb. Moreover, in samples coincubated with 0.2% Triton X-100 treatment, two Hb peaks were noted at 541 and 576 nm (Supplementary Fig. S1D). These two characteristic peaks were also apparent in samples with HPβ-CD–induced hemolysis. In samples treated with β-lap·HPβ-CD, however, a new peak was observed at 628 nm that was absent in samples treated with Triton X-100, HPβ-CD, and β-lap micelles. Both the shift in the Hb λ_{max} at 408 nm and the appearance of the new peak at 628 nm are indicative of conversion of the ferrous (Fe^{2+}) form of Hb to a ferric (Fe^{3+}) form known as methemoglobin (27–29), a conversion that is absent in β-lap micelles.

The pharmacokinetics of β-lap micelles were examined in mice bearing A549 NSCLC xenografts. The blood concentration of β-lap micelles was prolonged over a 24-hour time span, with a distribution phase half-life ($t_{1/2,\alpha}$) of 2 hours and an elimination half-life ($t_{1/2,\beta}$) of 28 hours (Fig. 3A). β-Lap micelles had a slow clearance rate, ~2 mL/h/kg. After 24 hours, ~20% of the initial dose was still present in the blood. Tissue distributions of β-lap micelles were measured at 2 and 24 hours after i.v. injection in organs including the liver, spleen, lungs, heart, kidneys, muscle, brain, and tumor (Fig. 3B). The largest accumulation of β-lap micelles was found in the spleen after 2 hours, with ~5.8% of the injected dose per gram tissue (% ID/g). β-Lap micelles also accumulated in the liver and kidneys but to a lesser extent, with 3.4% and 1.1% ID/g, respectively. In contrast, relatively minor levels of β-lap micelles were observed in other organs, including the heart, lungs, and muscle, 2 hours after injection. Conversely, significant β-lap micelle accumulation was noted in tumor tissue, reaching a level of ~1.5% ID/g. These levels remain relatively constant over prolonged times, as 1.6% ID/g β-lap micelles were found in tumor tissue at 24 hours. Micelle accumulation decreased slightly over time in organs such as the lungs, heart, and kidney 24 hours after injection. In contrast, the level of β-lap micelles in liver and spleen increased from 2 to 24 hours, reflecting lower blood circulation and their role as main clearance routes for β-lap micelles (Fig. 3B).

To examine the potential toxicity of micelle carriers due to increased RES uptake, we performed histologic analyses of liver, spleen, and kidney and compared the results with HPβ-CD. The spleen, kidney, and liver were affected to a greater degree in the HPβ-CD carrier group than in the micelle carrier group (Supplementary Fig. S3). The spleens in the HPβ-CD carrier group had extensive extramedullary hematopoiesis with abundant megakaryocytes in the red pulp and subcapsular region. This phenomenon was not observed in the micelle carrier group. The HPβ-CD carrier group showed collapsed glomeruli affecting between 5% and ~15% of glomeruli. In contrast, the kidneys pertaining to the micelle carrier group were histologically unremarkable. Chronic inflammation was seen in the portal regions in livers of both groups, consisting primarily of lymphocytes. Portal inflammation was much greater in the HPβ-CD carrier group when compared with the micelle carrier group and was shown to extend to the central vein region.

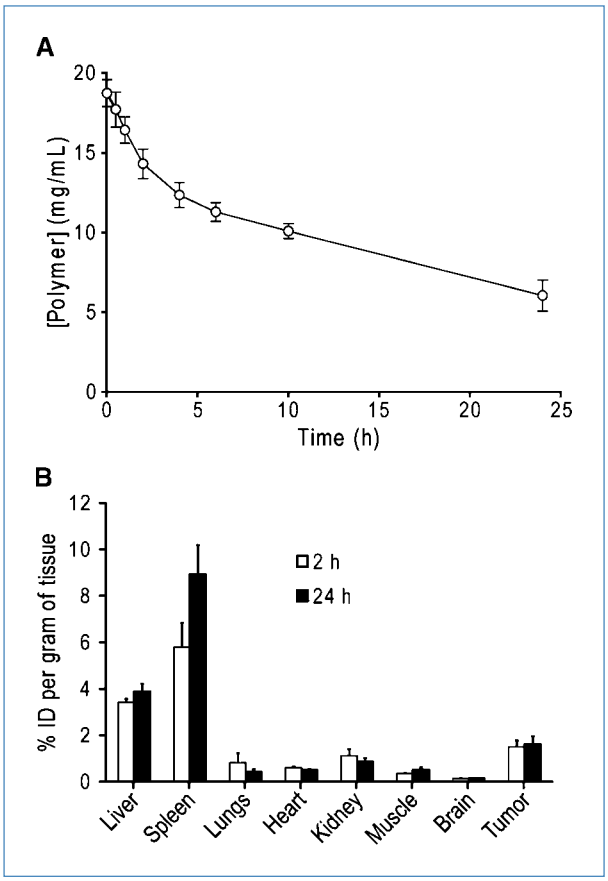

Figure 3. Pharmacokinetic analysis of β-lap polymer micelles (40 mg/kg) in female athymic nude mice bearing subcutaneous A549 NSCLC xenografts. A, blood concentration of β-lap micelles as a function of time. Pharmacokinetic parameters (e.g., $t_{1/2}$) were calculated using a two-compartment pharmacokinetic model (26). B, tissue distribution of β-lap micelles in various organs and tissues at 2 and 24 h after i.v. administration. All experiments were conducted in triplicate. Columns, mean (n = 3 for all organs except tumors, where n = 6); bars, SE.

Figure 4A shows the antitumor responses of subcutaneous A549 lung tumors treated with β-lap·HPβ-CD. The 30 mg/kg dose of β-lap·HPβ-CD proved rather ineffective at suppressing tumor growth, with only a slight improvement over the HPβ-CD vehicle control. Improved antitumor efficacy was noted at 40 mg/kg β-lap·HPβ-CD, especially at earlier

times of tumor growth. At day 9, HPβ-CD controls and 30 mg/kg β-lap·HPβ-CD measured 462 ± 151 mm^3 and 353 ± 39 mm^3, respectively. In contrast, tumors treated with 40 mg/kg β-lap·HPβ-CD measured 226 ± 15 mm^3, a minimal increase from its starting size of 210 ± 18 mm^3. After day 9 (completion of treatment), tumors in the 40 mg/kg β-lap·HPβ-CD group rapidly increased in size, nearly doubling to 404 ± 98 mm^3 by day 16. Kaplan-Meier survival data (Fig. 4B) show that 30 and 40 mg/kg doses of β-lap·HPβ-CD only resulted in 20% of mice surviving over the course of 100 days, with no statistical significance between 40 and 30 mg/kg β-lap·HPβ-CD or HPβ-CD alone groups.

In contrast to β-lap·HPβ-CD, all doses of β-lap micelles (30, 40, and 50 mg/kg) suppressed A549 NSCLC tumor growth from days 1 to 9 (Fig. 4C). More importantly, these doses did not result in any deaths during administration. At day 9, whereas control tumors reached a volume of 495 ± 125 mm^3, tumors treated with β-lap micelles measured 279 ± 51 mm^3, 268 ± 72 mm^3, and 149 ± 114 mm^3 at 30, 40, and 50 mg/kg, respectively. At 50 mg/kg β-lap micelles, tumor regression (from an initial volume of 224 ± 24 mm^3) was noted. After day 9, tumors in the 30 mg/kg group began to grow, reaching 500 ± 84 mm^3 by day 21. Tumors in mice treated with 40 mg/kg maintained volumes of ~300 mm^3 until day 21, after which the average volume was 306 ± 135 mm^3. Contrary to what was observed at equivalent doses in β-lap·HPβ-CD, 60% and 80% of animals treated with 30 and 40 mg/kg of β-lap micelles, respectively, survived 100 days. Animals receiving 50 mg/kg β-lap micelles resulted in the greatest efficacy and tumor regression, with tumors at days 14 and 21 measuring 170 ± 83 mm^3 and 152 ± 110 mm^3, respectively. Furthermore, Kaplan-Meier data (Fig. 4D) show that 50 mg/kg β-lap micelles significantly improved survival versus vehicle control ($P = 0.01$), with no lethality observed >100 days after treatment.

The antitumor efficacy of β-lap micelles was then investigated in a lung tumor model using athymic mice bearing orthotopic LLC tumors, a tumor cell line that undergoes NQO1-dependent cell death following β-lap administration *in vitro*. As can be seen from Supplementary Fig. S2, β-lap treatment of LLC tumors led to DNA damage, corroborated by alkaline comet assays, and subsequent PARP-1 hyperactivation

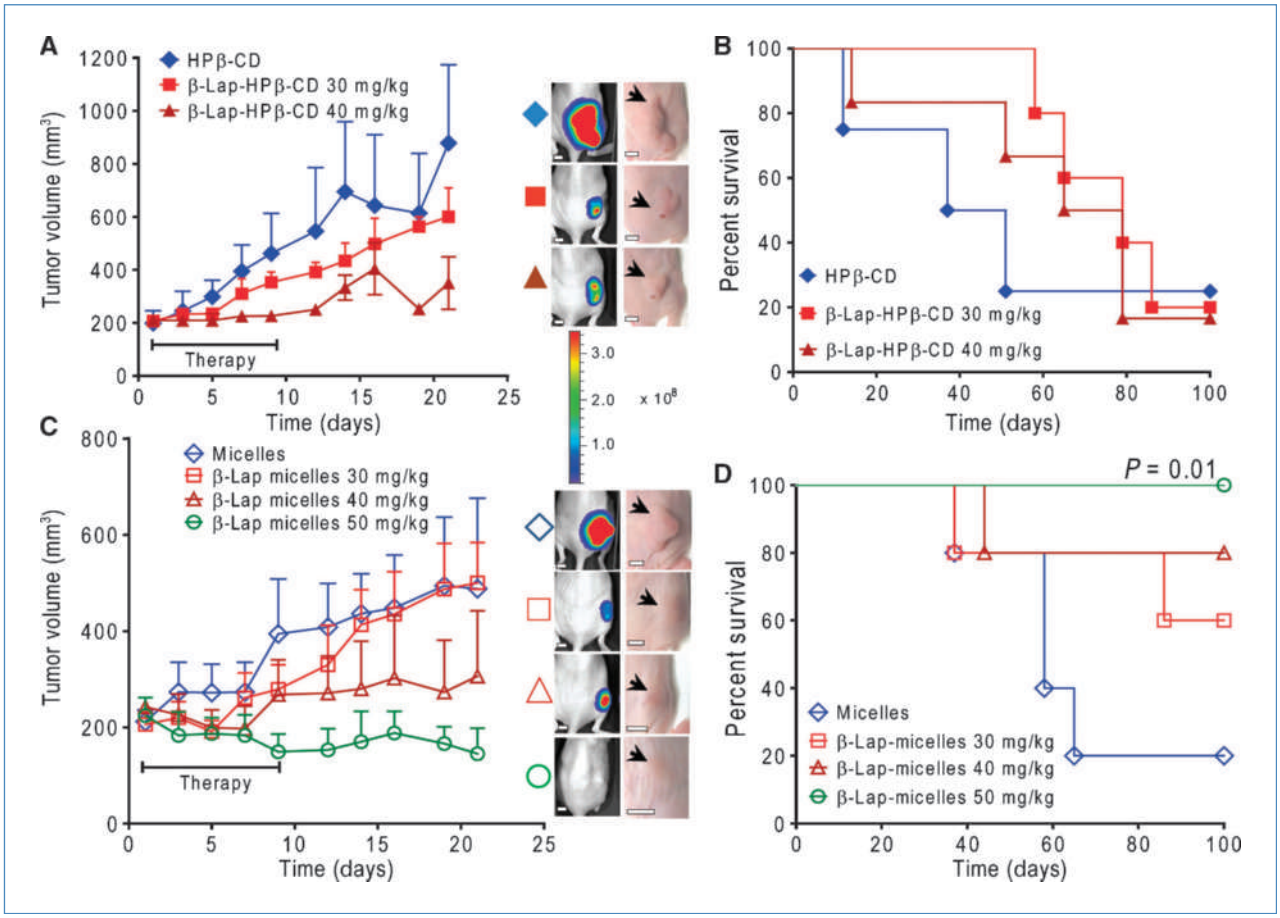

Figure 4. Evaluation of antitumor efficacy of β-lap micelles in female athymic nude mice bearing subcutaneous A549 NSCLC xenografts. Tumor growth inhibition (A) and Kaplan-Meier survival curve (B) of mice bearing subcutaneous A549 xenografts after 30 or 40 mg/kg of β-lap·HPβ-CD or HPβ-CD vehicle alone used as a negative control. Tumor growth inhibition (C) and Kaplan-Meier survival curve (D) of mice bearing subcutaneous A549 NSCLC xenografts after 30 to 50 mg/kg of β-lap micelles. PEG-PLA micelle alone was used as a negative control. For all treatment groups, i.v. administration every other day was performed for 9 d. Points, mean of three experiments with five mice per group; bars SE.

was indicated by PAR accumulation, as depicted in the Western blot. To gain further insight into the effect of β-lap micelles on disease progression, a separate study was performed in which BLI of mice was conducted throughout the course of treatment. Bioluminescence images of tumor growth in controls illustrate rapid tumor growth at day 9 (Fig. 5A), whereas β-lap micelle treatments resulted in significant tumor suppression. This was also evident on gross examination of control-treated and β-lap micelle–treated tumors, explanted at day 9. Lungs from control mice bore heavy tumor burdens compared with mice treated with β-lap micelles, with several pea-sized tumor nodules visible in controls, whereas few visible tumors were noted after β-lap micelle treatment. H&E analyses showed considerably increased tumor invasion throughout the lung parenchyma in control lungs compared with those of β-lap micelle–treated mice, corroborating the aforementioned survival, BLI, and tumor burden results. Indeed, on quantification (Fig. 5B), the tumor burden in lungs of control mice was more than double that noted in the lungs of mice treated with β-lap micelles (P = 0.01). Animal survival analysis shows that 50% of control animals died from disease at day 6, and all animals expired at day 7, confirming the aggressive nature of orthotopic LLC in athymic mice (Fig. 5C; ref. 30). In contrast, mice treated with 40 mg/kg β-lap micelles exhibited 50% death at day 9, with 5% surviving until day 17. Importantly, Kaplan-Meier curves indicate a statistically significant (P = 0.008) survival advantage with β-lap micelles over micelle carrier alone.

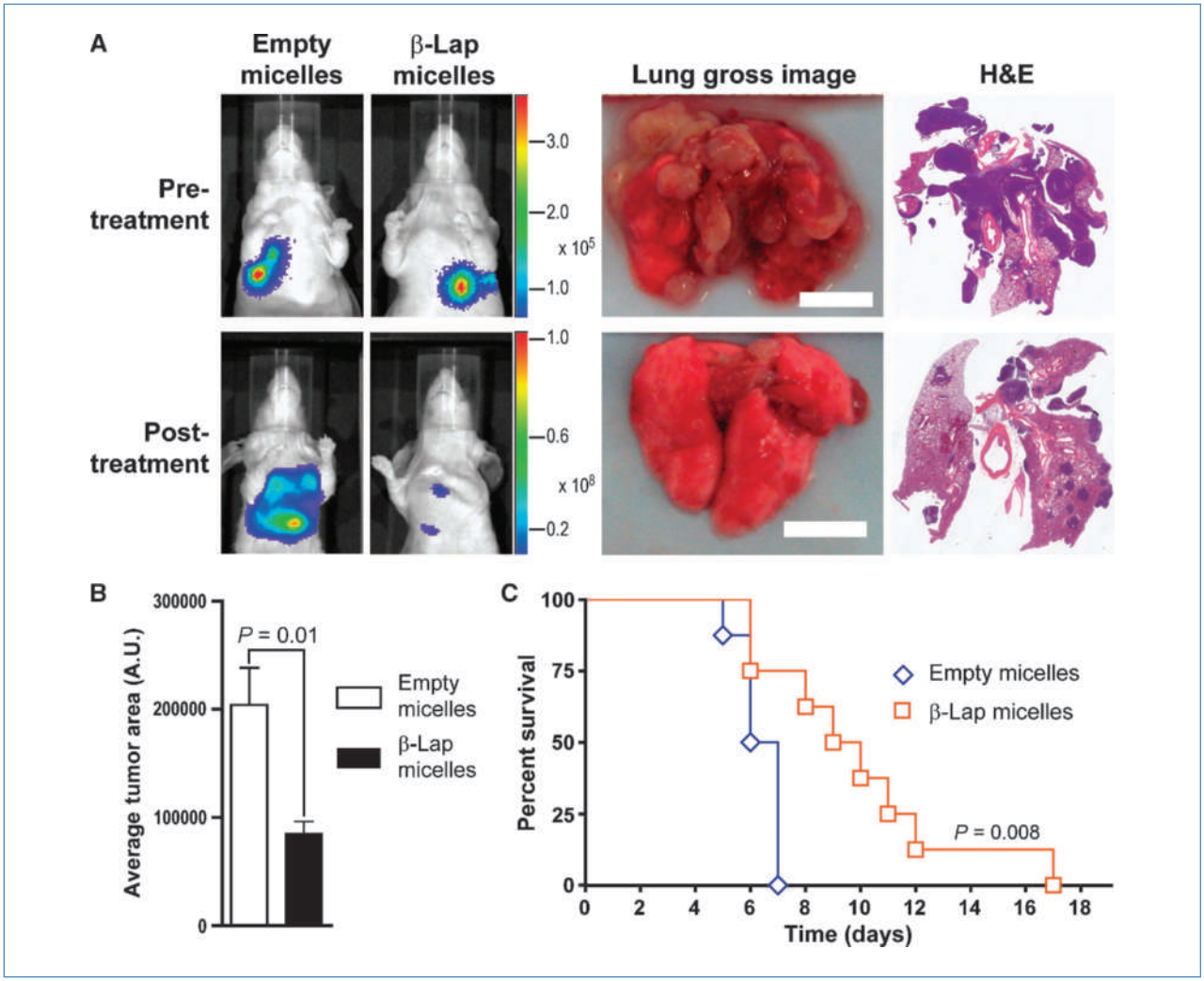

Figure 5. Evaluation of antitumor efficacy of β-lap micelles in female athymic nude mice bearing orthotopic LLC tumors. Micelle solutions were administered every other day for 9 d. A, bioluminescence images of mice before and after injection of either PEG-PLA micelles (vehicle alone) or β-lap micelles (treatment group). Gross images of lungs excised from mice treated with control micelles (*top*) or β-lap micelles (*bottom*) are depicted, as are histology (H&E) images of these explanted lungs. B, tumor burden present on explanted lungs (n = 3) from control-treated or β-lap micelle–treated tumors. C, Kaplan-Meier survival curve of female athymic nude mice (n = 8) treated with empty micelles or β-lap micelles at a dose of 40 mg/kg.

Discussion

In this study, β-lap micelles were proposed as a safe and efficacious nanotherapeutic strategy for the clinical translation of a promising anticancer agent. Although complexation was shown to dramatically increase its solubility and facilitated its clinical testing (8), various clinical trials reported that β-lap·HPβ-CD resulted in hemolytic anemia, significantly hindering its clinical potential (9). In this study, the complexation of β-lap and HPβ-CD proved hemolytic *in vitro*. β-Lap micelles, on the other hand, showed no evidence of hemolysis. In addition to hemolysis, β-lap·HPβ-CD also interacted with Hb, presumably by oxidation of the iron component of Hb (Fe^{2+} to Fe^{3+}). Such oxidation of iron is consistent with the known ROS generation by naphthoquinones (4). The mechanism by which β-lap converts the ferrous ion of Hb to methemoglobin is currently unclear but is hypothesized to involve metabolism of the drug by enzymes in RBCs (31). β-Lap can be metabolized into at least six distinct metabolites after incubation with RBCs (31), and ROS resulting from this metabolism may convert Hb to methemoglobin. Research is under way to investigate this mechanism and the *in vivo* consequences, as methemoglobinemia can lead to a decreased ability to carry oxygen, resulting in tissue hypoxia (28). Importantly, β-lap micelles are designed so that β-lap remains in the hydrophobic core of micelles, preventing drug interaction with RBCs and avoiding methemoglobinemia.

Prior studies showed that β-lap·HPβ-CD exhibited very short half-lives in blood, with an elimination phase half-life of ~24 minutes (unpublished results) and a clearance rate of 14 L/h/kg. The relatively weak binding affinity of β-lap with HPβ-CD (K_d = 1.1 × 10^{-3} mol/L; ref. 8) apparently leads to rapid β-lap·HPβ-CD dissociation following injection as well as even distribution to all organs. This pharmacokinetic profile is not therapeutically effective due to inadequate tumor accumulation and nonspecific toxicity to healthy tissues.

In the current study, ^{3}H-labeled PEG-PLA was used to measure the nanoparticle pharmacokinetics (32, 33). β-Lap micelles have prolonged circulation in blood, with an elimination phase half-life of 28 hours. The increased residence time of micelles in blood is beneficial for therapy, given that micelles can circulate longer, increasing the possibility of extravasation to tumor tissues during multiple passes. Consequently, we showed a comparatively higher accumulation of β-lap micelles in tumors over most normal tissues. This accumulation in tumors is most likely due to the EPR effect, or passive targeting, arising from the "leaky" vasculature of tumors (21, 22). It has been shown that fenestrations in tumor vasculature can be as large as 550 nm (34), a size that should allow for efficient extravasation of the 30-nm–sized β-lap micelles. Moreover, this deposition of micelles within the tumor seemed constant from 2 to 24 hours, suggesting impaired lymphatic drainage of tumor tissue (35). In addition to poor lymphatic drainage, micelle uptake and retention in tumor cells can also contribute to heightened and sustained accumulation over time. Savic and coworkers (36) examined the cell uptake of fluorescently labeled polymeric micelles and showed that micelles were internalized by endocytosis and distributed among several cytoplasmic organelles (e.g., lysosomes and endoplasmic reticulum). Taken together, our data suggest that β-lap micelles can effectively extravasate to, and remain within, tumors for prolonged times while exerting antitumor effects through drug release.

Results from this study show that β-lap·HPβ-CD administration to mice bearing subcutaneous NSCLC tumors failed to induce significant tumor growth delay or prolonged survival when compared with controls. Michaelis and colleagues (37) showed that a higher dose of a CD formulation of aphidicolin was necessary to match the efficacy of a low dose of a liposomal formulation of the drug. Similarly, Singla and colleagues (38) highlighted the disadvantages associated with paclitaxel-cyclodextrin formulations *in vivo*, stating that precipitation of the drug on blood dilution was a major deterrent to its clinical use. In light of these limitations, an alternate drug delivery strategy was necessary to fully harness the antitumor effects of β-lap. As hypothesized, β-lap micelles greatly improved not only animal safety and tolerability but also *in vivo* antitumor efficacy and animal survival, highlighting a distinct advantage over its cyclodextrin counterpart. When administered i.v., β-lap micelles effectively inhibited tumor growth compared with tumors treated with controls. When an orthotopic model was examined, β-lap micelles prolonged survival in an otherwise very aggressive tumor model. Previous results show that β-lap is effective against NSCLCs, such as A549 cells, which express threshold levels of NQO1, and kills irrespective of p53 and cell cycle status (3–6). This study validates the antitumor efficacy of β-lap micelles, a strategy that was shown to spare normal cells and tissues that express no or low levels of the enzyme. In spite of elevated accumulation in organs such as the liver and spleen, where indications of portal inflammation were present possibly due to elevated levels of NQO1 in the murine liver, β-lap micelles did not induce significant acute or chronic toxicity, as evidenced by tolerability (e.g., no weight loss) and prolonged survival of treated animals. Moreover, it is expected that β-lap micelles will result in low levels of toxicity in the human liver, where low levels of NQO1 are expressed (39, 40). Hence, improved efficacy of β-lap micelles was a result of both pharmacokinetic targeting of tumors through increased micelle accumulation and pharmacodynamic targeting of tumors overexpressing NQO1 by β-lap.

In summary, we highlight the clinical potential of a novel β-lap nanotherapeutic platform for the treatment of lung cancers with elevations in NQO1. Polymeric micelles prove a safe delivery platform for β-lap, allowing them to evade hemolytic anemia reactions, with reduced side effects and toxicity. Incorporation of the drug within micelles increased blood residence time, heightened tumor accumulation, and significantly lowered its toxicity. β-Lap micelles were highly efficacious in treating both subcutaneous and orthotopic lung tumors that overexpress NQO1. The unique integration of nanotechnology and NQO1 specificity should result in enhanced efficacy in future clinical applications.

Disclosure of Potential Conflicts of Interest

No potential conflicts of interest were disclosed.

Grant Support

NIH grants CA122994 (J. Gao) and CA102792 (D.A. Boothman) and Department of Defense postdoctoral fellowship W81XWH-04-1-0164 (C. Khemtong). E. Blanco is grateful for the support of a minority supplement grant from the NIH, as well as predoctoral Department of Defense grant (W81XWH-05-1-0258). E.A. Bey was supported by the Komen/AACR foundation and Simmons Comprehensive Cancer Center awards. BLI is facilitated by SW-SAIRP (U24 CA126688).

The costs of publication of this article were defrayed in part by the payment of page charges. This article must therefore be hereby marked *advertisement* in accordance with 18 U.S.C. Section 1734 solely to indicate this fact.

Received 10/29/2009; revised 02/15/2010; accepted 03/05/2010; published OnlineFirst 05/11/2010.

References

1. Jemal A, Siegel R, Ward E, Hao Y, Xu J, Thun MJ. Cancer statistics, 2009. CA Cancer J Clin 2009;59:225–49.
2. Belinsky M, Jaiswal AK. NAD(P)H:quinone oxidoreductase1 (DT-diaphorase) expression in normal and tumor tissues. Cancer Metastasis Rev 1993;12:103–17.
3. Pink JJ, Planchon SM, Tagliarino C, Varnes ME, Siegel D, Boothman DA. NAD(P)H:quinone oxidoreductase activity is the principal determinant of β-lapachone cytotoxicity. J Biol Chem 2000;275:5416–24.
4. Bey EA, Bentle MS, Reinicke KE, et al. An NQO1- and PARP-1- mediated cell death pathway induced in non-small-cell lung cancer cells by β-lapachone. Proc Natl Acad Sci U S A 2007;104:11832–7.
5. Bentle MS, Bey EA, Dong Y, Reinicke KE, Boothman DA. New tricks for old drugs: the anticarcinogenic potential of DNA repair inhibitors. J Mol Histol 2006;37:203–18.
6. Bentle MS, Reinicke KE, Dong Y, Bey EA, Boothman DA. Nonhomologous end joining is essential for cellular resistance to the novel antitumor agent, β-lapachone. Cancer Res 2007;67:6936–45.
7. Dong Y, Chin SF, Blanco E, et al. Intratumoral delivery of β-lapachone via polymer implants for prostate cancer therapy. Clin Cancer Res 2009;15:131–9.
8. Nasongkla N, Wiedmann AF, Bruening A, et al. Enhancement of solubility and bioavailability of β-lapachone using cyclodextrin inclusion complexes. Pharm Res 2003;20:1626–33.
9. Hartner L, Rosen L, Hensley M, et al. Phase 2 dose multi-center, open-label study of ARQ 501, a checkpoint activator, in adult patients with persistent, recurrent or metastatic leiomyosarcoma (LMS). J Clin Oncol 2007;25:20521.
10. Kawecki A, Adkins DR, Cunningham CC, et al. A phase II study of ARQ 501 in patients with advanced squamous cell carcinoma of the head and neck. J Clin Oncol 2007;25:16509.
11. Khong HT, Dreisbach L, Kindler HL, et al. A phase 2 study of ARQ 501 in combination with gemcitabine in adult patients with treatment naive, unresectable pancreatic adenocarcinoma. J Clin Oncol 2007;25:15017.
12. Li C, Nemunaitis J, Senzer N, et al. A phase Ib trial of ARQ 501, a selective checkpoint activator, in combination with docetaxel in patients with advanced solid tumors. J Clin Oncol 2006;24:13053.
13. Peer D, Karp JM, Hong S, Farokhzad OC, Margalit R, Langer R. Nanocarriers as an emerging platform for cancer therapy. Nat Nanotechnol 2007;2:751–60.
14. Ferrari M. Cancer nanotechnology: opportunities and challenges. Nat Rev Cancer 2005;5:161–71.
15. Gabizon AA. Pegylated liposomal doxorubicin: metamorphosis of an old drug into a new form of chemotherapy. Cancer Invest 2001;19:424–36.
16. Lee CC, MacKay JA, Frechet JM, Szoka FC. Designing dendrimers for biological applications. Nat Biotechnol 2005;23:1517–26.
17. Blanco E, Kessinger CW, Sumer BD, Gao J. Multifunctional micellar nanomedicine for cancer therapy. Exp Biol Med (Maywood) 2009; 234:123–31.
18. Sutton D, Nasongkla N, Blanco E, Gao J. Functionalized micellar systems for cancer targeted drug delivery. Pharm Res 2007;24:1029–46.
19. Torchilin VP. Structure and design of polymeric surfactant-based drug delivery systems. J Control Release 2001;73:137–72.
20. Haag R. Supramolecular drug-delivery systems based on polymeric core-shell architectures. Angew Chem Int Edit 2004;43:278–82.
21. Hashizume H, Baluk P, Morikawa S, et al. Openings between defective endothelial cells explain tumor vessel leakiness. Am J Pathol 2000;156:1363–80.
22. Maeda H. The enhanced permeability and retention (EPR) effect in tumor vasculature: the key role of tumor-selective macromolecular drug targeting. Adv Enzyme Regul 2001;41:189–207.
23. Planchon SM, Wuerzberger S, Frydman B, et al. β-Lapachone-mediated apoptosis in human promyelocytic leukemia (HL-60) and human prostate cancer cells: a p53-independent response. Cancer Res 1995;55:3706–11.
24. Shuai X, Ai H, Nasongkla N, Kim S, Gao J. Micellar carriers based on block copolymers of poly(ε-caprolactone) and poly(ethylene glycol) for doxorubicin delivery. J Control Release 2004;98:415–26.
25. Blanco E, Bey EA, Dong Y, et al. β-Lapachone-containing PEG-PLA polymer micelles as novel nanotherapeutics against NQO1-overexpressing tumor cells. J Control Release 2007;122:365–74.
26. Khemtong C, Kessinger CW, Ren J, et al. *In vivo* off-resonance saturation magnetic resonance imaging of αvβ3-targeted superparamagnetic nanoparticles. Cancer Res 2009;69:1651–8.
27. Kannan TR, Baseman JB. Hemolytic and hemoxidative activities in *Mycoplasma penetrans*. Infect Immun 2000;68:6419–22.
28. Lee J, El-Abaddi N, Duke A, Cerussi AE, Brenner M, Tromberg BJ. Noninvasive *in vivo* monitoring of methemoglobin formation and reduction with broadband diffuse optical spectroscopy. J Appl Physiol 2006;100:615–22.
29. Matsui M, Nakahara A, Takatsu A, Kato K, Matsuda N. *In situ* observation of reduction behavior of hemoglobin molecules adsorbed on glass surface. IEICE Trans Electron 2006;E89-C:1741–5.
30. Doki Y, Murakami K, Yamaura T, Sugiyama S, Misaki T, Saiki I. Mediastinal lymph node metastasis model by orthotopic intrapulmonary implantation of Lewis lung carcinoma cells in mice. Br J Cancer 1999;79:1121–6.
31. Yang RY, Kizer D, Wu H, et al. Synthetic methods for the preparation of ARQ 501 (β-lapachone) human blood metabolites. Bioorg Med Chem 2008;16:5635–43.
32. Liu J, Zeng F, Allen C. *In vivo* fate of unimers and micelles of a poly(ethylene glycol)-block-poly(caprolactone) copolymer in mice following intravenous administration. Eur J Pharm Biopharm 2007;65:309–19.
33. Yamamoto Y, Nagasaki Y, Kato Y, Sugiyama Y, Kataoka K. Long-circulating poly(ethylene glycol)-poly(D,L-lactide) block copolymer micelles with modulated surface charge. J Control Release 2001; 77:27–38.
34. Jain RK, di Tomaso E, Duda DG, Loeffler JS, Sorensen AG, Batchelor TT. Angiogenesis in brain tumours. Nat Rev Neurosci 2007;8:610–22.
35. Maeda H, Wu J, Sawa T, Matsumura Y, Hori K. Tumor vascular permeability and the EPR effect in macromolecular therapeutics: a review. J Control Release 2000;65:271–84.
36. Savic R, Luo L, Eisenberg A, Maysinger D. Micellar nanocontainers distribute to defined cytoplasmic organelles. Science 2003;300:615–8.
37. Michaelis M, Zimmer A, Handjou N, Cinatl J, Cinatl J, Jr. Increased systemic efficacy of aphidicolin encapsulated in liposomes. Oncol Rep 2005;13:157–60.
38. Singla AK, Garg A, Aggarwal D. Paclitaxel and its formulations. Int J Pharm 2002;235:179–92.
39. Radjendirane V, Joseph P, Lee YH, et al. Disruption of the DT diaphorase (NQO1) gene in mice leads to increased menadione toxicity. J Biol Chem 1998;273:7382–9.
40. Cresteil T, Jaiswal AK. High levels of expression of the NAD(P)H:quinone oxidoreductase (NQO1) gene in tumor cells compared to normal cells of the same origin. Biochem Pharmacol 1991;42:1021–7.